

Optical Absorption Spectra of Electrically Gated Bilayer Graphene

Li Yang¹

¹*Department of Physics, Washington University, St. Louis, Missouri, 63130, USA*

(Dated: November 15, 2018)

The electronic structure and optical response of electrically gated bilayer graphene are studied by first-principles approaches. We have obtained the induced band gap that is in good agreement with experiment when the applied electric field is less than 1.5 V/nm. The infrared optical absorbance is calculated within the single-particle excitation picture and its fine structures are presented. In addition, the calculated infrared optical absorbance is found to be strongly depending on stacking styles of bilayer graphene and the polarization direction of the incident light, which provides efficient ways to identify the electric-field intensity and stacking styles in experiment. Finally, many-electron effects are discussed.

PACS numbers: 73.22.Pr, 78.67.Wj

I. INTRODUCTION

Graphene, a single-layer graphite, is known for its unique electronic structure that has a massless Dirac-fermion dispersion close to the Fermi level [1–4]. This special feature results in many unusual properties [5, 6], e.g., quantum-Hall effect [3], Kohn anomaly [7, 8] and universal infrared optical conductance [9–15], etc.. In addition to the importance of fundamental physics, the high mobility of free carriers and 2-dimensional (2-D) nature of graphene make it possible to obtain high-performance microelectronic circuit structures, which could dramatically simplify the fabrication of devices and lower the cost consequently. However, despite above outstanding properties, one obstacle to applications of graphene is its zero-gap band structure. As a result, electrical conduction cannot be turned off using control voltages, which is essential for the operation of transistors [16].

Recent experiments have confirmed that an external electric field perpendicularly applied to bilayer graphene (BLG) can modify the electronic structure and induce a finite band gap by breaking the lattice inversion symmetry without degrading the high mobility [17–19]. Moreover, the induced band gap can be efficiently tuned in a wide range, up to a few tenths of an eV by the applied field around 1–2 V/nm [20, 21]. This discovery makes BLG the first known material with a wide-range tunable band gap. On the other hand, many theoretical studies have been performed to reveal the band structure of electrically gated BLG [22–27]. However, there are very few first-principles calculations about its optical absorption spectrum although a number of relevant experiments are using optical approaches to study BLG [20, 21] and corresponding tight-binding (TB) models [28] have been developed. Therefore, a first-principles calculation about the optical response of BLG is of great interest to the graphene community.

Beyond explaining available experimental data, we are motivated to study polarization effects of the optical response of electrically gated BLG because low-dimensional materials usually display quite different optical response to the incident light with different polarization directions

[29–33]. Therefore, the optical absorption spectra by different polarization directions may provide useful information to detect atomic and electronic structures of BLG [34]. Unfortunately, to date we have very limited first-principles knowledge about the polarization dependence of the infrared optical absorbance of electrically gated BLG. Finally, the stacking style of BLG is another interesting topic affecting its infrared optical response because different stacking styles result in different band structures around the Dirac point [35]. In particular, experimental conditions, such as external strain, imperfections and edges, can potentially induce different stacking styles locally [36]. Since it is not easy to identify the stacking style of BLG in experiment, the optical measurement may provide an efficient way to solve this problem.

Motivated by above considerations, we have performed first-principles calculations to study the electronic structure and optical absorption spectra of AA and AB stacked BLG with an perpendicularly applied electric field. Our DFT-calculated band gap is in good agreement with experimental measurements when the applied electric field is weak. Correspondingly, this induced band gap results in a significant modification of optical absorption spectra of BLG within the infrared frequency regime. Our calculation reveals that not only absorption peak positions but also their amplitudes and lineshapes are significantly changed by the applied field. In addition, electrically gated BLG displays strong polarization effects and a dependence of stacking styles, which are useful for its future electronic and photonic applications.

The remainder of this paper is organized as follows: in section II, we introduce the calculation details and structure of electrically gated BLG; in section III, the band gap of electrically gated BLG and comparisons with experimental measurements are presented; in section IV, we carry out detailed calculations on optical absorption spectra of electrically gated BLG with different stacking styles and polarization directions; in section V, many-electrons effects on infrared optical absorption spectra are discussed; in section VI, we summarize our studies and conclusion.

II. STRUCTURE AND CALCULATION DETAILS

Our calculations are using density functional theory (DFT) within the local density approximation (LDA) [37, 38] and the computational package is Quantum ESPRESSO [39]. The calculations are done in a supercell arrangement [40] with a plane-wave basis using norm-conserving pseudopotentials [41] with an 80 Ry energy cutoff. The distance between BLG sheets in neighboring supercells is set to be 2.0 nm to avoid spurious interactions. Two valence bands and two conduction bands are included to obtain converged optical absorption spectra up to 6 eV. A saw-tooth shape of electric potential is perpendicularly applied to mimic the gating electric field. A $128 \times 128 \times 1$ k-point grid is used to ensure converged DFT results. In this work, we focus on isolated BLG with fixed chemical potential, although the applied field can also be used to modify the chemical potential and induces a substantial change of optical absorption spectra [42]. Thus the optical response is studied by calculating the imaginary part of the dielectric function [43]

$$\varepsilon_2(\omega) = \frac{16\pi e^2}{\omega^2} \sum_{v,c} |\vec{\lambda} \cdot \langle v | \vec{v} | c \rangle|^2 \delta(\omega - (E_c - E_v)), \quad (1)$$

where $|v\rangle$ and $|c\rangle$ are valence and conduction states, respectively, \vec{v} is the velocity operator and $\vec{\lambda}$ is the polarization direction of the incident light.

However, the quantity of above imaginary dielectric function cannot be compared with experiments directly because its value is depending on the choice of the supercell size. In order to eliminate this artificial effect, we obtain the polarizability per unit area of BLG by [44]

$$\alpha_2(\omega) = (\varepsilon(\omega) - 1)d/4\pi, \quad (2)$$

where d is the distance between adjacent BLG sheets in our supercell arrangement. Moreover, most of experimental measured quantities are the optical absorbance. If we assume isolated BLG surrounded by infinite vacuum, the optical absorbance can be derived as [45]

$$A(\omega) = \frac{4\pi\omega}{c} \alpha_2(\omega) = \frac{16\pi e^2 d}{\omega c} \sum_{v,c} |\vec{\lambda} \cdot \langle v | \vec{v} | c \rangle|^2 \delta(\omega - (E_c - E_v)). \quad (3)$$

The other challenge of this study is how to obtain an optical absorbance with a good energy resolution. Because available experiments can only induce a small band gap of BLG in an order of a few tenths of an eV [19–21], we have to use an extremely dense k-point sampling to obtain comparable optical absorption spectra. Fortunately, we are interested in the infrared optical absorption spectrum up to 1 eV and only need to extensively sample the k-space around the Dirac point. In this study, we use a 100×100 k-point grid to sampling the mini first Brillouin zone (BZ) (0.1×0.1 of the first BZ) around the Dirac point, which is equivalently a 1000×1000 k-point

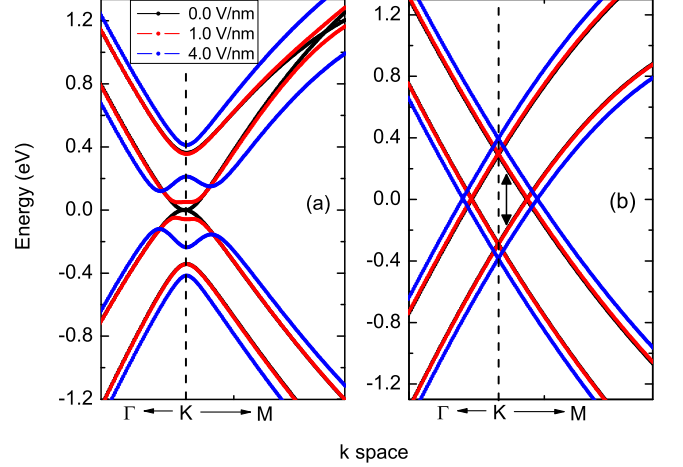


FIG. 1: (Color online) Band structure of electrically gated BLG close to the Dirac point. The AB stacked one is shown in (a) and AA stacked one is shown in (b).

sampling of the whole first BZ. This extremely dense sampling makes it possible to obtain a fine structure of optical absorption spectra with a 20 meV energy resolution.

Finally, we have considered two stacking styles of BLG, AB and AA. All these electrically gated structures are fully relaxed according to the atomic force and stress with DFT/LDA. We find that the applied electric field has minor effects on the structure of BLG. The relaxed inter-layer distance and C-C bond length are nearly identical under different electric fields up to 4 V/nm. The relaxed inter-layer distance of AB stacked BLG is 0.335 nm and that of AA stacked one is 0.346 nm, respectively, which are consistent with previous first-principles results [46].

III. BAND GAPS OF ELECTRICALLY GATED BLG

Plotted in Fig. 1 is the band structure of BLG close to the Dirac point calculated by DFT/LDA. In the absence of gating field, for AB stacked one shown in Fig. 1 (a), the valence band and conduction band touch each other with a quadratic shape due to breaking the AB symmetry by inter-layer interactions. Moreover, dispersions of valence bands and conduction bands are not symmetric to each other according to the Dirac point [47]. In particular, the lowest two conduction bands are even crossing each other along the K-M direction. This may induce impacts on optical absorption spectra of doped BLG [42]. For AA stacked BLG shown in Fig. 1 (b), the inter-layer interaction does not change the band dispersion but shifts Dirac points.

When gating electric field is applied, a finite band gap

is generated in AB stacked BLG. It can be understood by the following Hamiltonian describing the electronic structure near the Dirac point of AB stacked BLG [48],

$$H = \begin{pmatrix} \Delta & -\frac{\hbar^2}{2m}(k_x - ik_y)^2 \\ -\frac{\hbar^2}{2m}(k_x + ik_y)^2 & -\Delta \end{pmatrix} \quad (4)$$

where k is the momentum and Δ is the onsite energy difference between two layers of BLG, respectively. In the absence of electric field, $\Delta = 0$, thus the above effective Hamiltonian will lead to a gap-less quadratic band dispersion. When gating electric field is applied, it will introduce different onsite energies of two layers. Then the non-zero Δ will give rise to a finite band gap with a size of 2Δ . However, how to obtain the value of Δ is not easy because the applied electric field is inevitable to be screened by electrons in graphene, which can significantly depress the difference of onsite energy between graphene layers and reduce the band gap. DFT/LDA may be a better choice because it includes a part of screening effects through first-principles ways.

In Fig. 1 (a), as the intensity of the applied electric field increases, the band gap is enlarged and the band structure is no longer quadratic and finally replaced by a Mexican-hat shape dispersion. In addition to the induced band gap, the dispersion of conduction bands is modified by the applied field as well. For example, the lowest two conduction bands are no longer crossing each other along the K-M direction under strong applied field. On the contrary, the bottom of the second lowest conduction band and the top of the second highest valence band are not so sensitive to the applied electric field, and a significant change of these bands shows up until the applied field is larger than 4 V/nm.

We summarize our calculated band gap under different electric fields into Fig. 2. Previous self-consistent TB [28] and *ab initio* calculations [23] and experimental measurements [20] are plotted together for comparison. Interestingly, our calculated band gap is larger than previous *ab initio* calculations [23] and in good agreement with experimental measurements when gating field is less than 1.5 V/nm. For example, the previous DFT calculated band gap under a 0.5 V/nm field is around 30 meV, but our calculation provides a 50 meV gap, an over 60% enlargement. A larger energy cutoff and denser k-grid used in our calculations may be reasons for the difference between ours and the previous calculation [23]. We have checked some other first-principles studies and find that they are consistent with our results [26, 27]. For example, following Ref. [26], the band gap of BLG is 37 meV when the applied field is 0.45 V/nm, which is very close to our result. In Ref. [27], they get a band gap around 100 meV when the applied electric field is 1 V/nm, which is consistent with our data as well. For larger electric field (> 1.5 V/nm), our calculated band gap is approaching previous *ab initio* results [23] and significantly smaller than experimental measurement.

The reason for the consistence and inconsistency of our

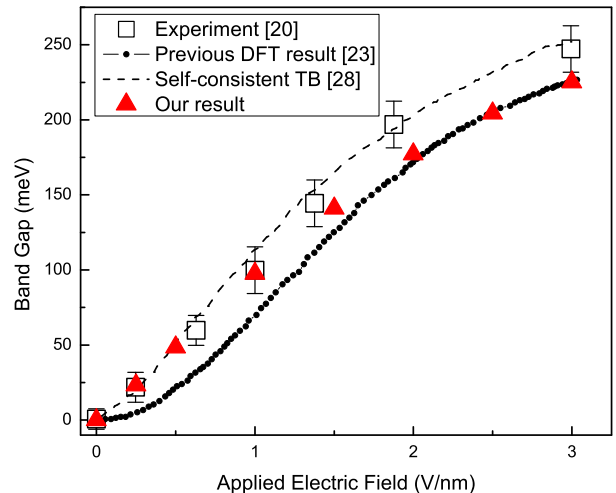


FIG. 2: (Color online) Electric-field dependence of the tunable band gap in AB stacked BLG. The experimental measurements and tight-binding and previous *ab initio* results are retrieved from Fig. 4 of Ref. [20].

calculated band gap with experimental data is complicated because DFT is known for its failure to obtain accurate band gaps of semiconductors [49]. In particular, there are studies supporting that self-energy corrections may enlarge the band gap of BLG [26, 45]. Here we attribute this “partial success” of DFT to experimental reasons, such as substrate effects. In experiment, BLG is sandwiched between gates, which may significantly enhance the screening between electrons. Thus this factor can reduce self-energy corrections from many-electron effects and makes DFT results close to experimental measurements. However, when the band gap is large enough as the applied field is more than 1.5 V/nm, substrate effects come to be smaller than self-energy corrections and our DFT result starts to significantly underestimate the band gap as shown in Fig. 2. Another potential reason for the above agreement between DFT gaps and optical gaps may be from the cancellation between self-energy corrections and excitonic effects [32]. More accurate experiments and first-principles calculations with many-electron effects included are expected to verify our discussions.

The band structure of AA stacked BLG close to the Dirac point is presented in Fig. 1 (b). Because inversion and AB symmetries are kept, we do not observe any finite band gap even when the applied electric field is around 4 V/nm. However, we do see an enlargement of the separation between two Dirac points marked in Fig. 1 (b), which is a result from the enhancement of the difference of onsite energy of two layers due to gating field. This small but essential change of band structure will result in corresponding modifications of optical absorption spectra and will be discussed in the next section.

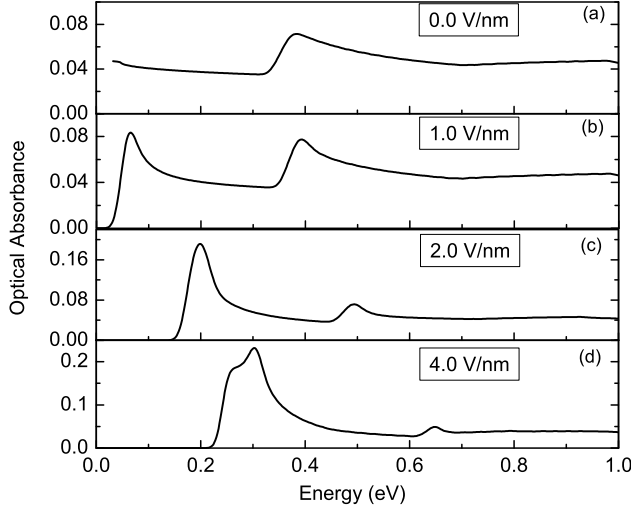


FIG. 3: (Color online) Optical absorbance of AB stacked BLG with applied gating electric field: (a) 0.0 V/nm, (b) 1.0 V/nm, (c) 2.0 V/nm and (d) 4.0 V/nm. The polarization of incident light is parallel to the graphene sheet. A 10 meV Gaussian broadening is applied to all plots. Please pay attention to the different scale of the above absorbance under different applied field.

IV. OPTICAL ABSORPTION SPECTRA OF ELECTRICALLY GATED BLG

First, we will focus on optical absorbance of AB stacked BLG with the incident light polarized parallel to the graphene sheet. The calculated optical absorption spectra are presented in Fig. 3. The optical absorption with a frequency less than 40 meV is not plotted because intra-band transitions and Drude factors are important there while we do not include them in this study. In Fig. 3 (a), plotted is the optical absorbance of AB stacked BLG in the absence of electric field. There is only one absorption peak around 400 meV that is due to inter-band transitions between the highest valence band and the second lowest conduction band and the second highest valence band and the lowest conduction band, respectively. Besides this optical absorption peak, the rest part of the absorbance is around 4.7 % that is consistent with previous experimental observations [13, 14].

When gating electric field is applied, a new absorption peak shows up because of the induced finite band gap, as shown in Fig. 3 (b), (c) and (d). By measuring the position of the sharpest slope of the new absorption peak, we identify that these values are consistent with our calculated band gap. Moreover, as applied electric field is stronger, the lineshape of the first absorption peak changes as well. For example, in Fig. 3 (d), the first absorption peak is actually a combination of a few peaks. From Fig. 1 (a), we can understand the origin of the change of the absorption lineshape is from the

Mexican-hat band structure under strong applied field. These changes of band dispersions and correspond optical absorption spectra will modify the effective mass of free carriers and are important to transport and electro-optical properties of BLG.

It has to be paid attention to that not only the peak position but also the peak intensity is modified by the applied electric field; larger field induces a stronger absorption peak. Plotted in Fig. 4 is the corresponding joint density of states (JDOS), which is helpful to understand the modification of the absorbance. As shown in Fig. 4 (a), the applied electric field not only induces a finite band gap but also gives rise to an enhanced peak at the band edge of the JDOS. This enhancement of the JDOS increases the absorbance intensity because more inter-band transitions are available within the certain frequency regime.

When turning to the second absorption peak, we find a weaker field dependence, which agrees well with our band structure conclusion because the second highest valence band and the second lowest conduction band are not sensitive to the applied field. Therefore, the shift of this peak is not prominent until the applied electric field is larger than 2.0 V/nm. Unlike the first absorption peak whose intensity is significantly enhanced, the intensity of the second peak does not change much under different applied fields.

In low-dimensional structures, the optical response is strongly depending on the polarization direction of the incident light. In BLG, we find the similar phenomenon. In Fig. 5, we present the optical absorbance of the incident light with a polarization direction perpendicular to the graphene sheet. First, the optical absorbance in this case is around two orders of magnitude smaller than that in Fig. 3. This depolarization effect is interesting and quite different from those observed in other nanostructures [30–32]. In those studies, we have to include the local field factor to obtain the depolarization effect that is not considered in this study yet.

Second, we see more fine structures from this perpendicular polarization case. For example, we observe the absorption peaks originated between the second highest valence band and the second lowest conduction band in Fig. 5 which is not shown in Fig. 3. Therefore, the energy position of these two relevant bands can be measured by perpendicularly polarized optical absorption spectra. Moreover, the intensity of the first absorption peak shows a stronger dependence on applied field than that of parallel-polarized cases. For example, its absorbance increases from 0.03% to 0.3% as the field changes from 0.5 V/nm to 4 V/nm. Therefore, although the magnitude of the absorbance is much smaller than that of Fig. 3, it provides stronger contrast if advanced experimental techniques can detect them, which may give better accuracy to identify the band structure.

Although AB stacked BLG is theoretically more stable than AA stacked one, it is interesting to study the optical response of the later one because the strain, im-

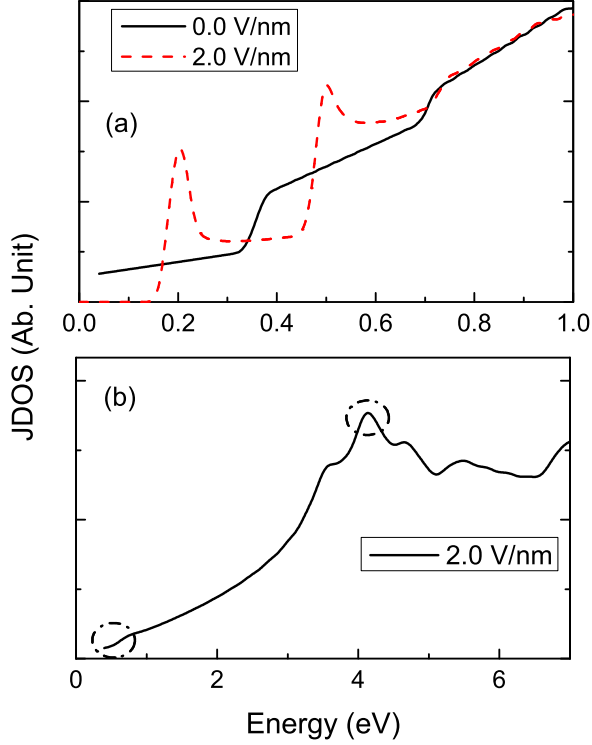


FIG. 4: (Color online) The JDOS of bare and electrically gated BLG (AB stacked). (a) The JDOS from 0 to 1 eV; (b) the JDOS from 0 to 7 eV. A 10 meV Gaussian broadening is applied to (a) and 100 meV Gaussian broadening is applied to (b).

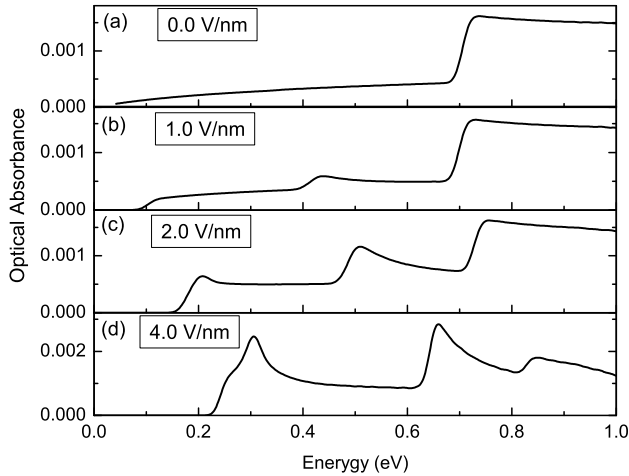


FIG. 5: (Color online) Optical absorbance of BLG (AB stacked) with applied gating electric field: (a) 0.0 V/nm, (b) 1.0 V/nm, (c) 2.0 V/nm and (d) 4.0 V/nm. The polarization of incident light is perpendicular to the graphene sheet. A 10 meV Gaussian broadening is applied to all plots. Please pay attention to the different scale of the above absorbance under different applied field.

perfections and grain boundaries may result in locally AA stacked BLG. Therefore, we have calculated the optical absorbance of AA stacked BLG and presented them in Fig. 6. Because of different symmetries, the AA stacked BLG shows a very different optical response from that of AB stacked one. In Fig. 6 (a), when the incident light is polarized parallel to the graphene sheet, the optical absorbance is zero within the frequency range up to 0.6 eV. This symmetry gap is due to the zero-oscillator strength between transitions from the highest valence band to the lowest conduction band [50]. Beyond that, the optical absorption is contributed from transitions between the highest valence band and the second lowest conduction band and the second highest valence band and the lowest conduction band, respectively. Interestingly, the optical absorbance above 0.6 eV is nearly a constant ($\sim 4.7\%$) that is the same as that of AB stacked BLG. Therefore, the universal infrared optical conductance of BLG above 0.6 eV is not sensitive to whether AA or AB stacking style.

Finally, the electric-field effect on the optical response of AA stacked BLG is weak as shown in Fig. 6. A significant shift of the absorption edge does not show up until the applied electric field is larger than 2 V/nm, which is consistent with our band structure calculations shown in Fig. 1 (b).

The polarization effect in AA stacked BLG is also quite different from that of AB stacked one. As shown in Fig. 6 (b), the magnitude of the optical absorbance for the polarization direction perpendicular to the graphene sheet is comparable to that with a parallel polarization while a significant depolarization effect are observed in AB stacked BLG. However, since the local field effect may depress the perpendicularly polarized optical absorption spectrum, a significant change of Fig. 6 (b) may happen after including many-electron effects. Interestingly, when we compare the optical absorbance with the corresponding JDOS that is shown in Fig. 6 (c), we find the perpendicularly polarized optical absorbance has a similar peak structure around 0.6 eV as that of the JDOS. This fact suggests that perpendicularly polarized absorbance is a better choice to measure the JDOS in AA stacked BLG.

V. EXCITONIC EFFECTS ON INFRARED OPTICAL ABSORPTION SPECTRA

It is known that many-electron effects, like electron-hole interactions [51, 52], are of importance in determining the optical response of low-dimensional carbon materials [53–56]. In particular, a previous first-principles calculation with many-electron effects included has revealed enhanced electron-hole interactions in the optical absorption spectrum of BLG around 5 eV [45]. Therefore, questions to our DFT-calculated infrared optical absorption spectra are if many-electron effects will play an important role there and if they will qualitatively change our result for BLG with a finite band gap.

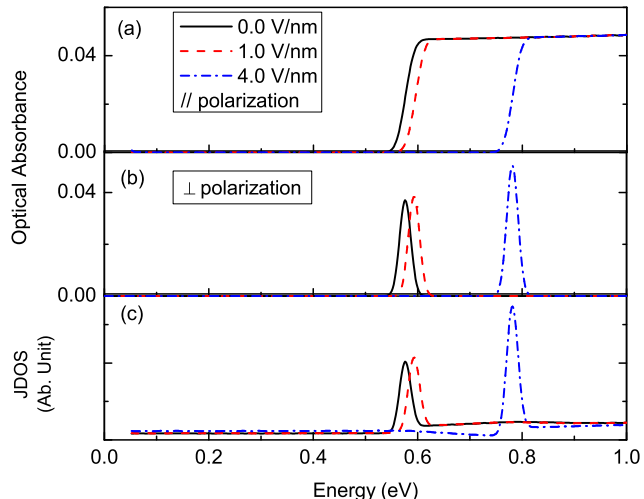


FIG. 6: (Color online) Optical absorbance and JDOS of AA stacked BLG under different gating electric field. (a) Optical absorbance with parallel polarized incident light; (b) optical absorbance with perpendicularly polarized incident light; (c) JDOS. A 10 meV Gaussian broadening is applied to all plots.

Usually, there are two important factors to dictate excitonic effects on the optical response of solids. One is the screening between electrons and holes; a smaller band gap means a stronger screening and weaker electron-hole interactions. The other one is the number of available electron-hole pair configurations within a certain energy regime. Within the Tamm-Dancoff approximation [57], an exciton state can be written as

$$\chi_S(x_e, x_h) = \sum_k \sum_v \sum_c^{hole\ elec} A_{vck}^S \psi_{c,k}(x_e) \psi_{v,k}^*(x_h), \quad (5)$$

where A_{vck} is the exciton amplitude, $\psi_{c,k}(x_e)$ and $\psi_{v,k}(x_h)$ are the electron and hole states, respectively. From this formula, it is easy to see that a stronger bound exciton state needs more electron-hole pair configurations to form a localized state. Therefore, flatter bands are preferred to form enhanced excitonic effects, which is consistent with the hydrogenic model because larger effective mass gives rise to a stronger binding energy of excitons accordingly.

For electrically gated BLG, an important consideration

is the small number of available electron-hole pair states within the infrared frequency regime because of the sharp slope of band dispersion close to the Dirac point of BLG. In Fig. 4 (b), we have marked the JDOS around the band gap and the peak around 4 to 5 eV. Since the JDOS around the induced band gap is much smaller than that around 4 to 5 eV, we expect excitonic effects around the band gap is much smaller than those around 4 to 5 eV. However, since the induced band gap is relatively small, excitons with a small binding energy (a few tenths of an eV) can modify optical spectra [58] although they will not significantly change main conclusions of our calculation. To justify this open question about the excitonic effects in electrically gated BLG, more accurate first-principles studies are necessary, which are beyond this paper. In addition, we suggest future experiments to be performed by measuring the lineshape of absorption peaks as what had been done in metallic Carbon nanotubes [59] to check the existence of bound excitons in electrically gated BLG.

VI. SUMMARY

In conclusion, we have performed first-principles calculations on the electronic structure and optical absorption spectra of electrically gated BLG. The electric-field dependence of band gaps is evaluated. Our calculated result is partially in good agreement with recent experiments. We believe self-energy corrections are important although experimental substrate effects can depress it when the applied field is weak.

The optical absorbance is calculated within the single-particle transition picture. Absorption peaks, lineshapes and intensity are found to be strongly depending on the applied electric field. The polarization effect of the incident light and stacking styles of BLG are studied as well, which provide efficient ways to detect the atomic and electronic structure of BLG. Finally, excitonic effects are discussed and possible experiments are suggested to verify our calculations.

ACKNOWLEDGMENTS

We thank Cheol-Hwan Park and Anders E. Carlsson for fruitful discussions. Computational resources are provided by Lonestar of Teragrid at the Texas Advanced Computing Center .

[1] K.S. Novoselov, et al., *Science* **306**, 666 (2004).
[2] K.S. Novoselov, et al., *Nature* **438**, 197 (2005).
[3] Y. Zhang, Y.-W. Tan, H.L. Stormer, P. Kim, *Nature* **438**, 201 (2005).
[4] C. Berger, et al., *J. Phys. Chem. B* **108**, 19912 (2004).
[5] A.K. Geim and K.S. Novoselov, *Nature Materials* **6**, 183 (2007).

[6] A.H. Castro Neto, et al., *Rev. Mod. Phys.* **81**, 109 (2009).
[7] S. Piscanec, et al., *Phys. Rev. Lett.* **93**, 185503 (2004).
[8] M. Lazzeri and F. Mauri, *Phys. Rev. Lett.* **97**, 266407 (2006).
[9] T. Ando, Y.S. Zheng, and H. Suzuura, *J. Phys. Soc. Jpn.* **71**, 1318 (2002).
[10] V.P. Gusynin and S.G. Sharapov, *Phys. Rev. B*, **73**,

- 245411 (2006).
- [11] N.M.R. Peres, F. Guinea, and A.H. Castro Neto, Phys. Rev. B **73**, 125411 (2006).
 - [12] J.M. Dawlaty, et al., arXiv:cond-mat/0801.3302.
 - [13] R.R. Nair, et al., Science **320**, 1308 (2008).
 - [14] K.F. Mak, et al., Phys. Rev. Lett. **101**, 196405 (2008).
 - [15] A.R. Wright, F. Liu, and C. Zhang, Nanotechnology **20**, 405203 (2009).
 - [16] M.I. Katsnelson, K.S. Novoselov and A.K. Geim, Nature Phys. **2**, 620 (2006).
 - [17] T. Ohta, et al., Science, **313**, 951 (2006).
 - [18] J.H. Chen, et al., Nature Nanotechnology, **3**, 206 (2008).
 - [19] J.B. Oostinga, et al., Nature Mater., **7**, 151 (2008).
 - [20] Y. Zhang, et al., Nature, **459**, 820 (2009).
 - [21] K.F. Mak, C.H. Lui, J. Shan, and T.F. Heinz, Phys. Rev. Lett., **102**, 256405 (2009).
 - [22] E.V. Castro, et al., Phys. Rev. Lett., **99**, 216802 (2007).
 - [23] H. Min, B. Sahu, S.K. Banerjee, and A.H. MacDonald, Phys. Rev. B, **75**, 155115 (2007).
 - [24] C.L. Lu, et al., Phys. Rev. B **73**, 144427 (2006).
 - [25] E.J. Nicol and J.P. Carbotte, Phys. Rev. B **77**, 155409 (2008).
 - [26] P. Gava, M. Lazzeri, A.M. Saitta, and F. Mauri, Phys. Rev. B **79**, 165431 (2009).
 - [27] B.R.K. Nanda and S. Satpathy, Phys. Rev. B **80**, 165430 (2009).
 - [28] L.M. Zhang, et al., Phys. Rev. B **78**, 235408 (2008).
 - [29] H. Ajiki and T. Ando: Physica B **201**, 349 (1994).
 - [30] C.D. Spataru, S. Ismail-Beigi, L.X. Benedict, and S.G. Louie, Appl. Phys. A **78**, 1129 (2004).
 - [31] E. Chang, G. Bussi, A. Ruini, and E. Molinari, Phys. Rev. Lett. **92**, 196401 (2004).
 - [32] L. Yang, C.D. Spataru, S.G. Louie, and M.Y. Chou, Phys. Rev. B **75**, 201304 (2007).
 - [33] C. Zhang, L. Chen and Z. Ma, Phys. Rev. B **77**, 241402 (2008).
 - [34] T. Ando and M. Koshino, J. Phys. Soc. Jpn. **78**, 104716 (2009).
 - [35] J.-C. Charlier, J.-P. Michenaud, and X. Gonze, Phys. Rev. B **46**, 4531 (1992).
 - [36] X. Jia, et al., Science **323**, 1701 (2009).
 - [37] P. Hohenberg and W. Kohn, Phys. Rev. **136**, B864 (1964).
 - [38] W. Kohn and L.J. Sham, Phys. Rev. **140**, A1133 (1965).
 - [39] S. Baroni et al., Quantum ESPRESSO: open-source package for research in electronic structure, simulation, and optimization, <http://www.quantum-espresso.org/> (2005).
 - [40] M.L. Cohen, M. Schlüter, J.R. Chelikowsky, and S.G. Louie, Phys. Rev. B **12**, 5575 (1975).
 - [41] N. Troullier and J.L. Martins, Phys. Rev. B **43**, 1993 (1991).
 - [42] F. Wang, et al., Science **320**, 206 (2008).
 - [43] M.L. Cohen and J.R. Chelikowsky, *Electronic Structure and Optical properties of Semiconductors* (Springer-Verlag, New York, 1988), 2nd ed.
 - [44] C.-H. Park, C.D. Spataru, and S.G. Louie, Phys. Rev. Lett., **96**, 126105 (2006).
 - [45] L. Yang, C.-H. Park, J. Deslippe and S.G. Louie, Phys. Rev. Lett. **103**, 186802 (2009).
 - [46] A.N. Kolmogorov and V.H. Crespi, Phys. Rev. B **71**, 235415 (2005).
 - [47] Z.Q. Li, et al., Phys. Rev. Lett. **102**, 037403 (2009).
 - [48] E. McCann, and V.I. Falko, Phys. Rev. Lett. **96**, 086805 (2006).
 - [49] M.S. Hybertsen and S.G. Louie, Phys. Rev. B **334**, 5390 (1986), and references therein.
 - [50] H. Min and A.H. MacDonald, Phys. Rev. Lett. **103**, 067402 (2009).
 - [51] W. Hanke and L.J. Sham, Phys. Rev. Lett. **43**, 387 (1979).
 - [52] M. Rohlfing and S.G. Louie, Phys. Rev. B **62**, 4927 (2000).
 - [53] C.D. Spataru, S. Ismail-Beigi, L.X. Benedict, and S.G. Louie, Phys. Rev. Lett. **92**, 077402 (2004).
 - [54] L. Yang, M.L. Cohen and S.G. Louie, Nano Lett **7**, 3112 (2007).
 - [55] D. Prezzi, et al., Phys. Rev. B **77**, 041404 (2008).
 - [56] L. Yang, M.L. Cohen and S.G. Louie, Phys. Rev. Lett. **101**, 186401 (2008).
 - [57] L.X. Benedict, E.L. Shirley, and R.B. Bohn, Phys. Rev. Lett. **80**, 4514 (1998); Phys. Rev. B **57**, 9385 (1998).
 - [58] C.-H. Park and S.G. Louie, Nano Lett. **10**, 426 (2010).
 - [59] F. Wang, et al., Phys. Rev. Lett. **99**, 227401 (2007).